

Change in Stiffness of Reinforced Concrete Tunnel Walls and Its Effect Under Fire Load

Zoltán MAJOR^a, Edina KOCH^{b,1} and Éva LUBLÓY^c

^a Department of Transport Infrastructure and Water Resources Engineering, Széchenyi István University, Egyetem tér 1., Győr 9026, Hungary

^b Department of Structural and Geotechnical Engineering, Széchenyi István University, Egyetem tér 1., Győr 9026, Hungary

^c Department of Construction Materials and Technologies, Faculty of Civil Engineering, Budapest University of Technology and Economics, Műegyetem rakpart 3., Budapest 1111, Hungary

ORCID ID: Zoltán Major <https://orcid.org/0000-0002-7677-5377>, Edina Koch <https://orcid.org/0000-0001-7623-8814>, Éva Lublóy <https://orcid.org/0000-0001-9628-1318>

Abstract. This article uses the knowledge gained from tunnel fires to address the structural analysis of tunnel walls during fire exposure. The designing at normal temperature and its theoretical background are discussed in the literature. As these books did not yet deal with the issue of fire protection designing, we tried to supplement the existing theoretical knowledge with the knowledge provided by the relevant standards for reinforced concrete tunnel walls. In addition, we have tried to add our own individual ideas to the theory where we felt that there were gaps. The theoretical summary has been compiled in such a way that it can be easily transferred and applied to everyday practice. In this article, we discuss in detail the calculation of the internal forces in tunnel walls during fire exposure. Due to space constraints, the issue of designing at normal temperatures is only touched upon in this article, limiting it to the knowledge available in the literature. Since finite element modelling has become a commonly used technique in tunnel design since the 1970s, we use its potential to investigate the effects of earth pressure and surface loads on the tunnel walls during fire and their changes, using specific software for geotechnical design. In accordance with the limitations of the scope, the determination of the equivalent thickness and the modulus of elasticity of the tunnel wall is also presented in order to determine the internal forces during the fire action.

Keywords. Reinforced concrete, tunnel wall, stiffness changing, fire load, finite element method

1. Introduction

During fire exposure, the structure must be designed in an extreme design condition. Accordingly, the simultaneity of each effect shall be considered according to Eq. (1) in [1].

$$\sum_{j \geq 1} G_{k,j} + P + A_d + \psi_{1,1} \times Q_{k,1} + \sum_{i > 1} \psi_{2,i} \times Q_{k,i} \quad (1)$$

¹ Corresponding Author: Edina Koch, E-mail: koche@sze.hu

where:

- G_k : characteristic value of the permanent load,
- P : representative value of the effect from tension,
- A_d : design value of the accidental effect (temperature change),
- $Q_{k,1}$: characteristic value of the dominant variable effect,
- $Q_{k,i}$: characteristic value of the i -th potential effect operating simultaneously with the dominant variable effect,
- $\psi_{1,1}$: combination factor for the frequent value of the highlighted variable effect,
- $\psi_{2,i}$: combination factors for the quasi-constant values of the additional possible impacts.

MSZ EN 1991-1-2 [2] states an important principle: if the fire resistance requirements are defined by the standard effect of fire, indirect effects transmitted from adjacent elements (inhibited deformation, effects due to inhibition of thermal expansion, etc.) need not be taken into account. In all other cases, however, particular attention should be paid to the following effects and their consequences:

- inhibited thermal expansion in structural elements;
- unequal temperature changes in statically indeterminate structures;
- non-uniform temperature distribution within the cross-section;
- thermal expansion of adjacent structural elements;
- the effect of thermal expansion of structural elements exposed to fire on the behaviour of structural parts outside the fire compartment.

If a detailed study is carried out treating the support structure as a complete unit, indirect thermal effects cannot be ignored. As the tunnel lining is tested as a complete unit and for non-standard fire exposure, it is necessary to consider the inhibited deflection as shown in Figure 1. In this case the accidental effect (A_d) is a time/temperature dependent quantity.

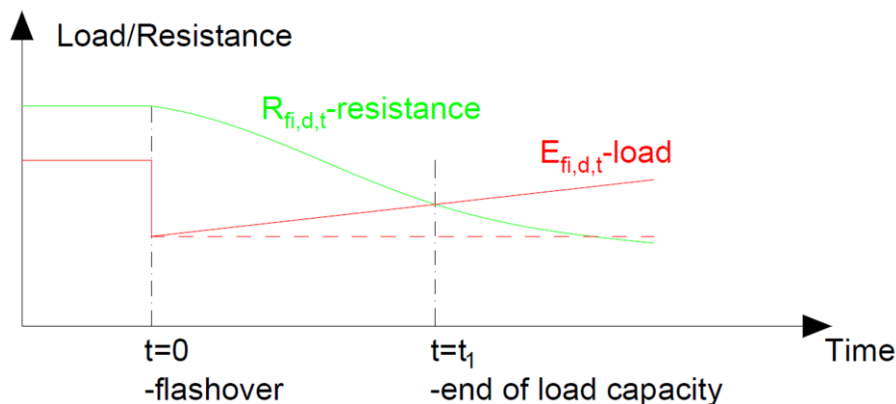


Figure 1. Verification of the strength requirements under fire-impact with inhibited deflection (Source: author's own illustration)

The application of Formula 1 requires special considerations in tunneling practice. In a research report [3] of the International Tunnelling Association (ITA-AITES), it was considered appropriate to investigate for the first time the load imposed on tunnel linings made of reinforced concrete segments in the ultimate limit state. The report takes into account the effects of earth pressure and groundwater in the discussed load combination 8, as shown in Eq. (2), where the original source notations are used.

$$1,25 \times (w + WA_p) + 1,35 \times (EH + EV) + 1,50 \times ES \quad (2)$$

where:

- w: characteristic value of the dead load,
- WA_p: characteristic value of groundwater pressure,
- EH: characteristic value of horizontal earth pressure,
- EV: characteristic value of vertical earth pressure,
- ES: characteristic value of the additional surface load.

By observing the combination according to Eq. (2), we conclude that these effects, without the application of combination factors, can, together with their base value, load the wall in an extreme design condition. If we add to the formula a term representing an accidental effect (A_d), then a load corresponding to Eq. (3) should be applied to the tunnel wall.

$$(w + WA_p) + (EH + EV) + ES + A_d \quad (3)$$

where the markings are the same as previously stated.

In special places where the wall is designed as a tunnel structure in tensioned soil, the effect of tensioning (P) should be added to Eq. (3).

Knowing the loads, the internal forces (normal force and bending moment) in the tunnel walls can be determined. Whichever method is chosen by the investigator, it should be borne in mind that the normal stiffness (EA) and the bending stiffness (EI) of the wall will be a time/temperature dependent quantity during the fire action. Their value decreases as the temperature increases. For concrete and reinforced concrete walls, the change in stiffness during fire is largely due to changes in the dimensions of the undamaged concrete cross-section and to a lesser extent to changes in the modulus of elasticity.

2. Materials

To determine the stresses caused by external loads, it is necessary to reduce the stiffness of the wall. This can also be investigated using finite element modeling [4-5]. The standard [6] offers designers a stiffness reduction according to Eq. (4) for a general column cross-section.

$$(EI)_z = [k_c(\theta_M)]^2 \times E_c \times I_z \quad (4)$$

where:

- (EI)_z: equivalent stiffness of the reduced concrete cross-section,
- k_c(θ_M): reduction factor for concrete strength at point M,
- E_c: modulus of elasticity of concrete at normal temperature,
- I_z: moment of inertia of the reduced cross-section.

Formula 4 can be applied to reinforced concrete tunnels as follows:

- the thickness of the wall should be taken into account in the calculation with the value h_{fi} (reduced wall thickness). The interpretation of the dimensions can be seen in Figure 2. The definition of the value is presented in the Methodology. In case of software calculation, this requires a modification of the model, while

in case of manual calculation, the bending stiffness (EI) and normal stiffness (EA) must be determined from this thickness.

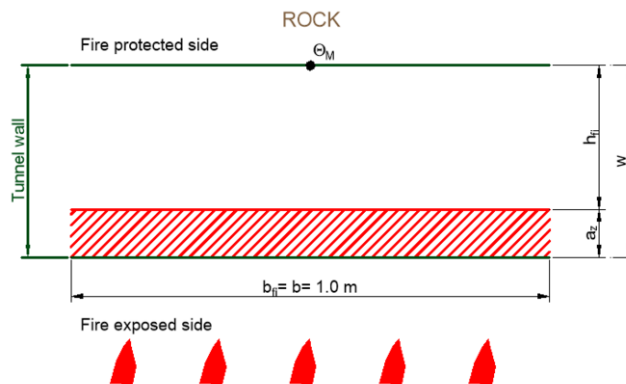


Figure 2. Explanation of dimensions (Source author’s own illustration)

- The stiffening effect of reinforcement, since it is typically not even taken into account in the ultimate limit state calculation, should also be ignored in the fire calculation.
- The modulus of elasticity of concrete ($E_{c,\theta}$) corresponding to θ_M (temperature at point M) is taken from Eq. (5), deriving it from Eq. (4).

$$E_{c,\theta} = [k_c(\theta_M)]^2 \times E_c \tag{5}$$

The inclusion of the concrete strength reduction factors $k_c(\theta_i)$ and $k_c(\theta_M)$ for normal concretes is based on the values in Table 1 (values up to a maximum temperature of 800 °C are shown) [6]. In our article, we focused on concrete with quartz aggregates.

Table 1. Concrete strength reduction factors for normal concretes and stress-strain diagram elongations [6]

Temperature °C	$f_{c,\theta} / f_{ck}$	$f_{c,\theta} / f_{ck}$	$\epsilon_{c1,\theta}$	$\epsilon_{cu1,\theta}$
	quartz aggregate	limestone aggregate	quartz and limestone aggregates	quartz and limestone aggregates
20	1.00	1.00	0.0025	0.0200
100	1.00	1.00	0.0040	0.0225
200	0.95	0.97	0.0055	0.0250
300	0.85	0.91	0.0070	0.0275
400	0.75	0.85	0.0100	0.0300
500	0.60	0.74	0.0150	0.0325
600	0.45	0.60	0.0250	0.0350
700	0.30	0.43	0.0250	0.0375
800	0.15	0.27	0.0250	0.0400

Based on laboratory tests, strength reduction factors can be determined for special cases and special concrete mixtures [7-8]. In this way, the effect of the materials that make up the concrete on the behavior of the concrete and the structure during fire can also be taken into account [9-11].

3. Methodology

The PLAXIS 2D geotechnical finite element model was used to model the fire effect. The reinforced concrete tunnel was embedded in loose sand. The hardening soil model with small strain stiffness was applied to describe the soil behavior [12]. The applied soil properties are summarized in Table 2. The effect of groundwater is neglected in the article, since its assumed depth does not influence the results. The reinforced concrete tunnel with a diameter of $d=5.5$ m was modeled by plate element (the initial thickness is 300 mm) and the wall was modeled with an elastic material model. The surface load is 24 kN/m^2 in the applied model.

Table 2. Soil properties [12]

γ_{unsat}	γ_{sat}	e_0	E_{50}^{ref}	$E_{\text{ur}}^{\text{ref}}$	m	c'	φ'	ψ	$\gamma_{0,7}$	G_0^{ref}	R_{inter}
kN/m^3	kN/m^3	-	MPa	MPa	-	kPa	$^\circ$	$^\circ$	-	MPa	-
20	20	0.5	24000	72000	0.58	1	33	3	1,6E-4	87200	0.7

The cross-section damaged by the fire must be replaced by a reduced cross-section, the damaged zone depth (a_z) of that thickness on the side exposed to the fire must be neglected [6]. The reduced wall thickness (h_{fi}) can be calculated based on Eq. (6). Its value continuously decreases with increasing temperature.

$$h_{fi} = w - a_z \quad (6)$$

Based on [6], the depth of the damaged zone can be determined based on Eq. (7), and the auxiliary quantity included in it can be determined based on Eq. (8).

$$a_z = w \times \left[1 - \left(\frac{k_{c,m}}{k_c(\theta_M)} \right)^{1,3} \right] \quad (7)$$

$$k_{c,m} = \frac{(1 - \frac{0,2}{n})}{n} \times \sum_{i=1}^n k_c(\theta_i) \quad (8)$$

where:

- $k_{c,m}$: mean value of the cross-section reduction factors,
- $k_c(\theta_i)$: the reduction factor for concrete strength at the centre line of each zone,
- $k_c(\theta_M)$: reduction factor for concrete strength at point M,
- n : number of parallel zones within the tunnel lining thickness w .

The calculation is detailed in [13]. The necessary theoretical foundations for this are summarized in [14]. The isotherms required for the practical calculation can be found in [15], the graphs valid for hydrocarbon fire curve are illustrated in Figure 3. The calculated input parameters are shown in Table 3.

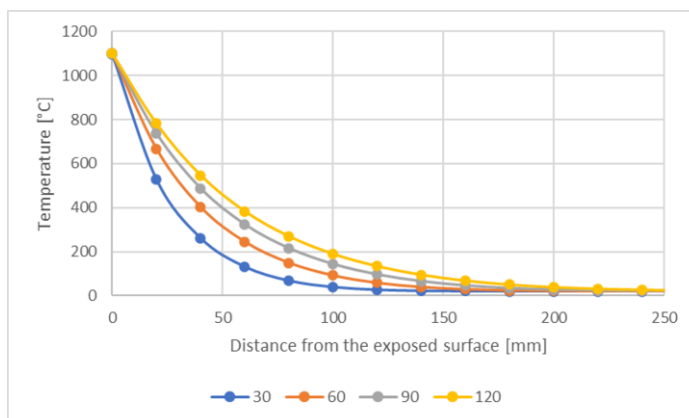


Figure 3. Temperature distribution for varying density and specific heat values with the lower limiting coefficient of thermal conductivity - hydrocarbon fire curve (Source: author's own illustration)

Table 3. Input parameters of the structure

	$t=$	0	30	60	90	120	min
initial wall thickness	$w=$	300	300	300	300	300	mm
damaged zone depth	$a_z=$	0	29	44	52	58	mm
reduced wall thickness	$h_{ri}=$	300	271	256	248	242	mm
wall width	$b=$	1000	1000	1000	1000	1000	mm
initial modulus of elasticity	$E_0=$	11600	11600	11600	11600	11600	N/mm ²
strength reduction factor at point M	$k_c(\Theta_M)=$	1	0.924	0.8858	0.8646	0.8471	-
modulus of elasticity at temperature Θ	$E_\Theta=$	11600	9904	9102	8671	8324	N/mm ²
wall thickness at time t	$w(t)=$	300	271	256	248	242	mm
normal stiffness at time t	$EA(t)=$	3480000	2683930	2330072	2150503	2014386	kN
bending stiffness at time t	$EI(t)=$	26100	16426	12725	11022	9831	kNm ²

The investigation can also be performed using other solutions, such as the hyperstatic reaction method (HRM) [16].

4. Results

PLAXIS 2D was used to determine the normal forces and bending moments in the crown, shoulders and invert of the tunnel based on the combination of the loads corresponding to Formula 3. The finite element mesh is shown in Figure 4. In our study, the analysis of accidental effects (inhibited deformation) was omitted. The results of the modelling are summarised in Table 4.

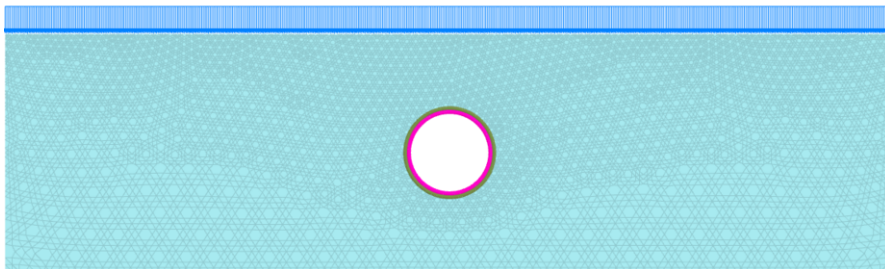


Figure 4. Finite element mesh of the model (Source: PLAXIS 2D)

Table 4. Internal forces in the tunnel wall under fire effect

t [min]		0	30	60	90	120
crown	N(t) [kN/m]	105.3	109.9	112.4	113.3	114.2
	M(t) [kNm/m]	52.18	38.99	32.55	29.2	26.66
shoulder	N(t) [kN/m]	251.4	242.4	238.3	236.0	234.4
	M(t) [kNm/m]	-48.33	-35.17	-29.2	-27.16	-25.06
invert	N(t) [kN/m]	108.8	110.9	111.4	112.0	112.7
	M(t) [kNm/m]	36.49	23.33	17.55	14.87	12.98

Based on Table 3, we determined the relative change in both normal and bending stiffness from $t=0$ and did the same for the normal force and moment values reported in Table 3 at the investigated locations. The relative normal force values as a function of relative normal stiffness are shown in Figure 5 while the relative bending moment values as a function of relative bending stiffness are shown in Figure 6. As can be seen from the figures, a linear functional relationship between the relative stiffnesses and the relative internal forces can be assumed in the case under consideration. The trend of change (increasing or decreasing) and the rate of change are different for each load (normal force, bending moment) and for the investigated locations (crown, shoulder, invert).

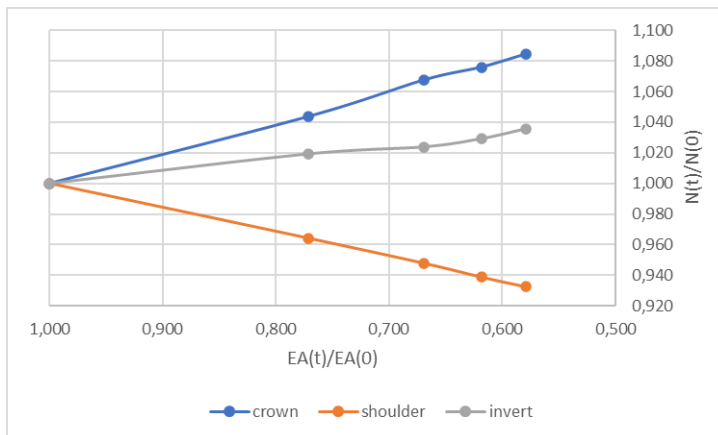


Figure 5. Variation of normal force as a function of variation of normal stiffness (Source: author's own illustration)

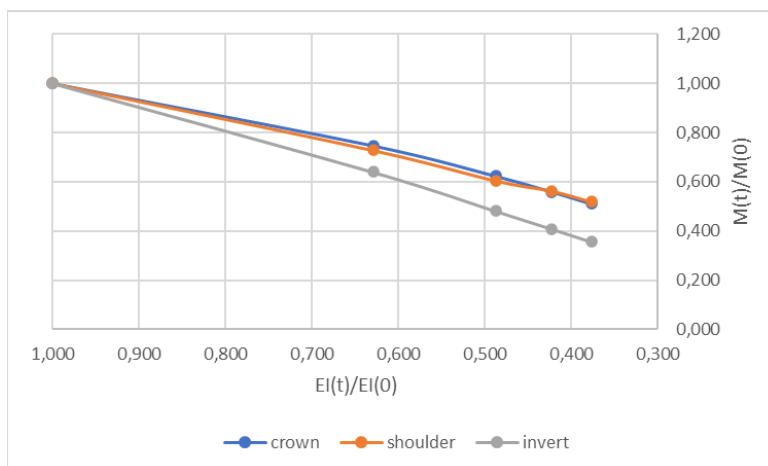


Figure 6. Variation of bending moment as a function of variation of bending stiffness (Source: author's own illustration)

The graphs shown in Figure 5 show that the resulting normal force is almost insensitive to changes in the normal stiffness. On the other hand, based on the graphs shown in Figure 6, it can be seen that the change in bending stiffness has a decisive effect on the bending moments.

In their article, the authors omitted the question of the use of fire protection. In their future research, they definitely want to investigate this by taking international results, fire protection materials and structural solutions into account [17-20].

5. Conclusions

In this article, the basic principles of fire-resistance design of tunnel wall have been described in details and a concrete example of the internal forces arising from external effects have been given. A linear relationship between the investigated quantities as a function of the relative stiffness of the wall was found. It is important to verify the linear change on additional models (other soil types, other structure). By this way, nomograms and auxiliary tables can be edited for easier work. Even based on existing results, we can create an opportunity to extrapolate from them. As the results showed, the fire effect typically causes a significant change in the bending moment. Based on the internal forces, we also consider it important to examine the stress level comparison, thus the effect of the two internal forces can be examined together.

References

- [1] Balázs LG et. al: Szerkezetek tervezése tűzterherre az MSZ EN szerint, PI Innovációs Kft., Budapest, 2010, ISBN: 978-615-5093-02-9 (in Hungarian)
- [2] MSZ EN 1991-1-2:2005 Eurocode 1: A tartószerkezeteket érő hatások. 1-2. rész: Általános hatások. A tűznek kitett szerkezeteket érő hatások. MSZT, Budapest, Hungary, 2005 (in Hungarian)
- [3] ITA Report n°22 - Guidelines for the Design of Segmental Tunnel Linings, ISBN 978-2-9701242-1-4, Avignon, 2019. https://about.ita-aites.org/files/WG2_-ITA-REPORT-DesignSegment.pdf.

- [4] Szép J, Movahedi Rad M, Habashneh M. Enhancing Fire-Resistant Design of Reinforced Concrete Beams by Investigating the Influence of Reliability-Based Analysis. *Eng Rep*, 2024;2:1–15. doi:10.1002/eng2.12879
- [5] Szép J, Habashneh M, Lógó J, Movahedi Rad M. Reliability Assessment of Reinforced Concrete Beams under Elevated Temperatures: A Probabilistic Approach Using Finite Element and Physical Models. *Sustainability*. 2023; 15(7):6077. doi:0.3390/su15076077
- [6] MSZ EN 1992-1-2:2013 Eurocode 2: Betonszerkezetek tervezése. 1-2. rész. Általános szabályok. Szerkezetek tervezése tűzhatásra. MSZT; Budapest, Hungary, 2013. (in Hungarian)
- [7] Szép J, Major Z, Szigeti C, Lublós É. The Impact of Cement Aggregates on the Fire Resistance Properties of Concrete and its Ecological Footprint. 2023; *Chem Eng Trans*, 2023;107:337–342. doi:10.3303/CET23107057
- [8] Lublós E. The relationship between concrete composition and structural stability in case of fire. *Constr Build Mater*. 2024; 431:136545. doi:10.1016/j.conbuildmat.2024.136545
- [9] Sándor F. The effect of concrete components on the residual split-tensile strength of concrete exposed to high temperature. In 1st Ybl Conference on the Built Environment – Book of Abstracts 2023 (p. 65).
- [10] Fehérvári S. Effect of cooling methods on the residual properties of concrete exposed to elevated temperature. *Results In Eng*. 2022;16:100797. <http://doi.org/10.1016/j.rineng.2022.100797>
- [11] Fehérvári S, Nehme SG. Effect of the cooling regime on the residual compressive strength of concrete. In *Proceedings-WTC Scandinavian way 2011, ITA AITES World Tunnel Congress “Underground spaces in the service of a sustainable society”*; 2011; p. 11.
- [12] Benz T, Vermeer PA, Schwab R. A small-strain overlay model. *Int J Numer Anal Met Geom*. 2009; 33:25-44. <https://doi.org/10.1002/nag.701>
- [13] Majorosné Lublós ÉE, Major Z. Alagútfalazatok termikus vizsgálata (4. rész) – Tartószerkezeti elemzés. *SÍNEK VILÁGA*. 2024; 66(1):11-23. (in Hungarian)
- [14] Majorosné Lublós ÉE, Major Z. Alagútfalazatok termikus vizsgálata (1 rész) - Elméleti alapok. *SÍNEK VILÁGA*. 2023; 3:14-23. (in Hungarian)
- [15] Majorosné Lublós ÉE, Major Z. Alagútfalazatok termikus vizsgálata (2. rész) – Gyakorlati ismeretek. *SÍNEK VILÁGA*. 2023; 65(5):2-8. (in Hungarian)
- [16] Du D, Dias D, Do NA. A Simplified Way to Evaluate the Effect of Temperature on a Circular Tunnel. *Geotechnics* 2021; 1, 385–401. doi: 10.3390/geotechnics1020018
- [17] Morgan Advanced Materials Inc. Tunnel Fire Protection [Brochure]. <https://www.morganthermalceramics.com/media/mhbfibv/tunnel-fire-protection.pdf>
- [18] ECO Tunneling Inc. Fire-protection in Tunnels [Brochure]. <https://irp.cdn-website.com/2e572db5/files/uploaded/ECO%20Tunneling%20Aestuver-compact-Tunnel---EN-lo.pdf>
- [19] Shuttleworth P. Fire protection of concrete tunnel linings. in: *The Third International Conference on Tunnel Fires and Escape from Tunnels*, 2001.
- [20] Miclea PC, Chow WK, Shen-Wen C, Junmei L, Kashef A, Kang K. International tunnel fire-safety design practices. *ASHRAE Journal*. 2007;49(8):50-60 <https://nrc-publications.canada.ca/eng/view/accepted/?id=4f73a655-690f-4865-b326-7edfd66ba6cb>